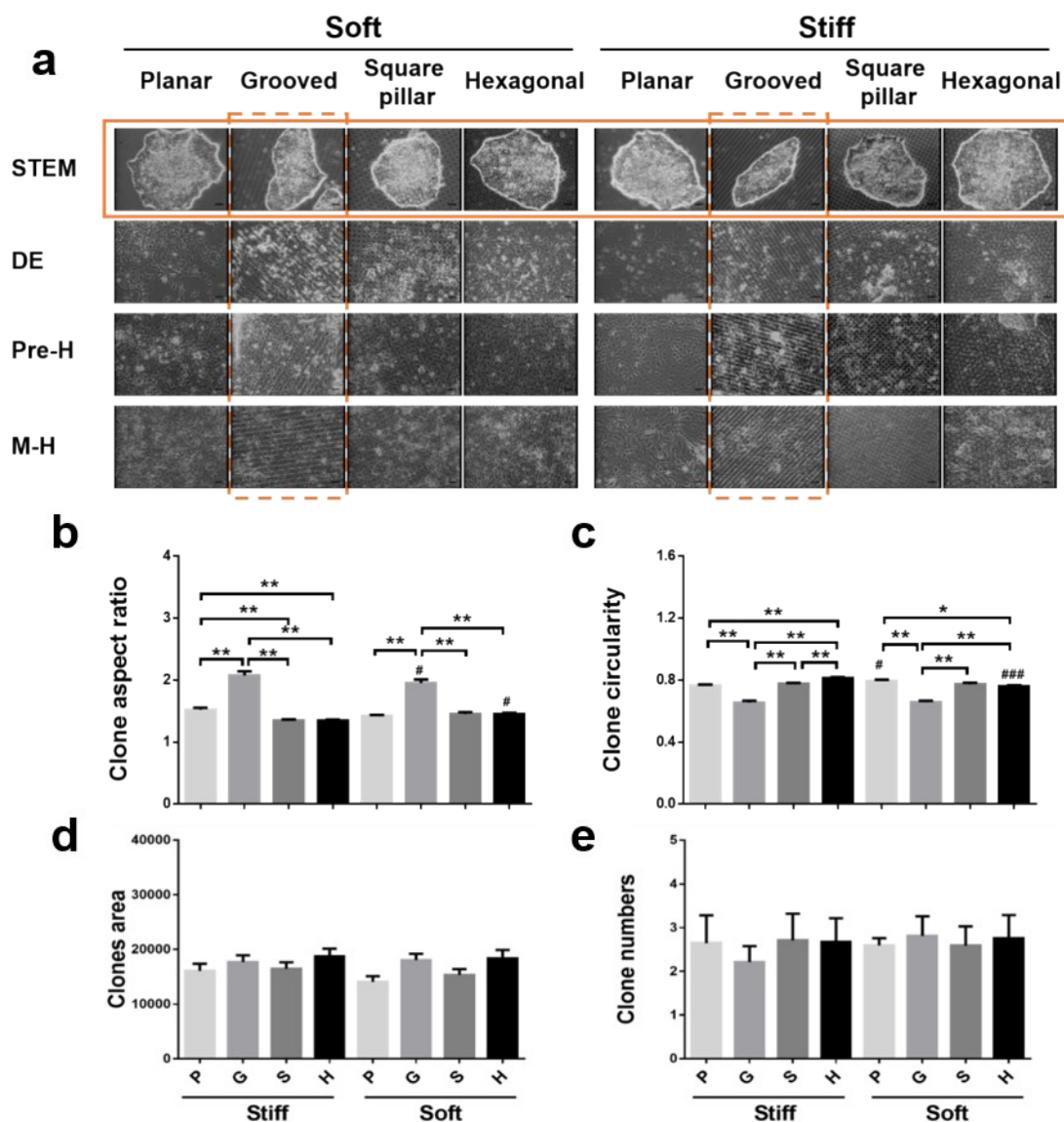
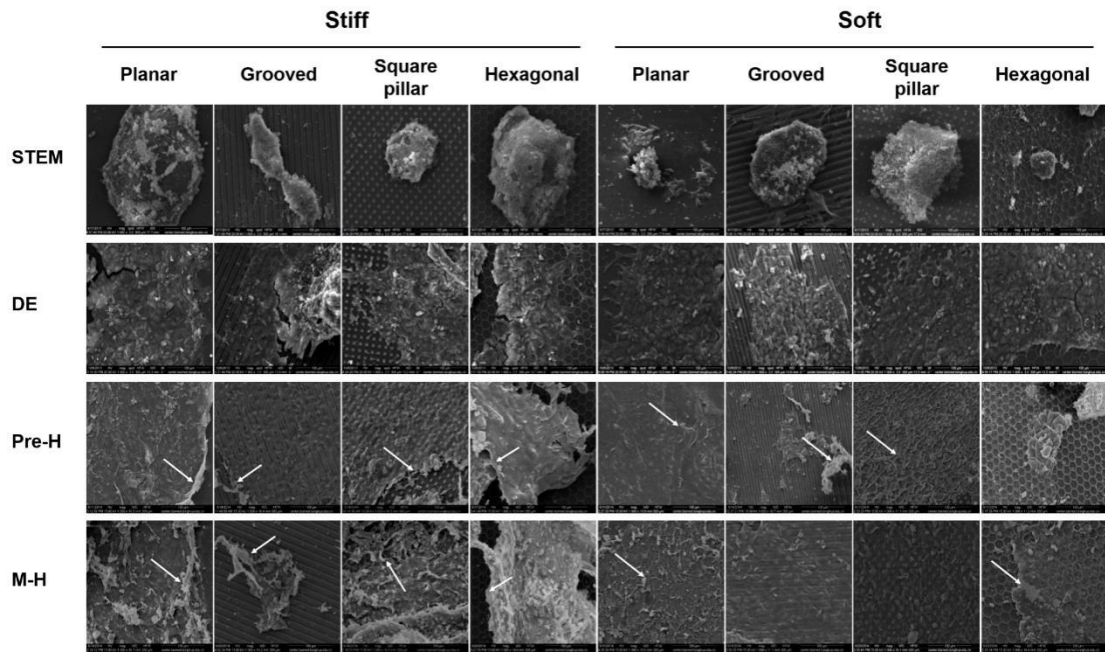


SUPPLEMENTARY FIGURES AND TABLES



**Figure S1.** Morphology of H1 cells on PA hydrogel. (a) Optical images of H1 cells on a topographical PA hydrogel pre-coated with 200 µg/ml collagen I in planar (*P*), grooved (*G*), square pillar (*S*), or hexagonal (*H*) configurations, illustrating their morphological changes from stem cells (STEM) through definitive endoderm (DE) and precursor hepatocytes (Pre-H) to hepatocyte-like cells (M-H) on soft (6.1 kPa) or stiff (46.7 kPa) substrates. Bar = 50 µm. *Dotted boxes* indicated the typical morphology on grooved PA gel. (B-E) Morphological analyses of H1 cells on topography- or stiffness-varied substrates. The aspect ratio (b), circularity (c), and projected area (d) of H1

clones were measured (as shown in the *solid box* in panel A) and the average number of clones per unit area was determined in each replicate (E). Data were presented as the mean  $\pm$  SE from triplicate repeats (totally >132 colonies). \* or \*\*,  $P < 0.05$  or  $0.01$  compared with the values between distinct topographies at same stiffness. # or ###,  $P < 0.05$  or  $0.001$  compared with the values between stiff and soft substrates in same configuration (two-way ANOVA).



**Figure S2.** SEM images of H1 cells differentiating into HLCs at the four stages. *Arrows* indicated the sites where ECM tended to be accumulated at the Pre-H or M-H stage.

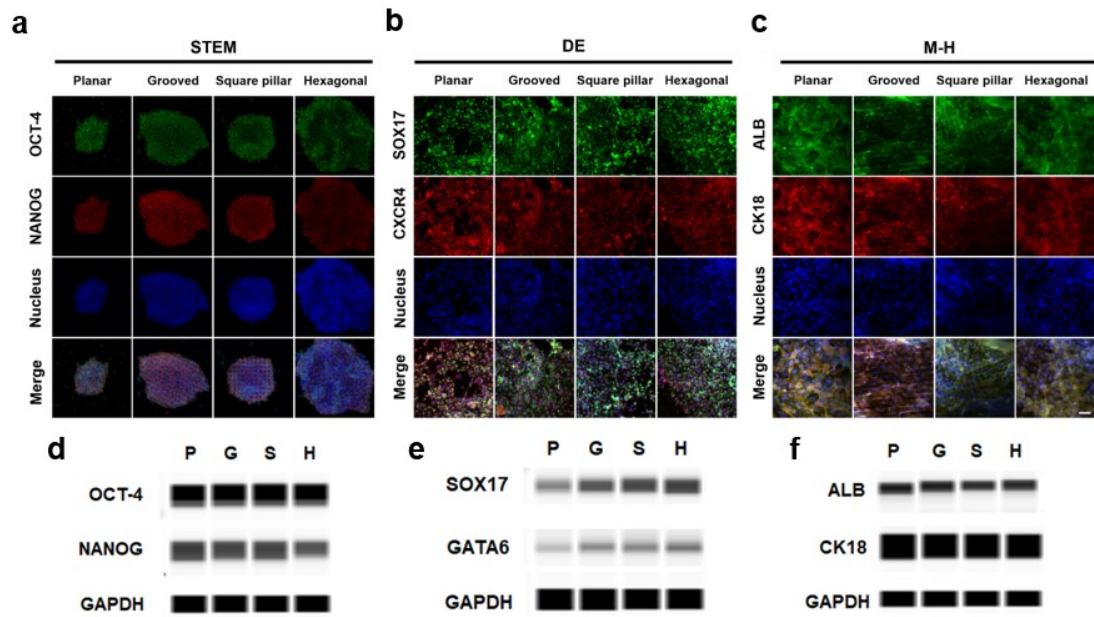


**Figure S3.** Biomarker expressions of H1 cells at different topographies on *stiff* PA gel. Typical immunostaining (*1<sup>st</sup> row*) or immunoblotting (*2<sup>nd</sup> row*) images of OCT-4 and NANOG (a, d), SOX17 and CXCR4 (or GATA6) (b, e), or ALB and CK18 (c, f) were illustrated at the STEM, DE or M-H stage. Bar = 50  $\mu$ m.

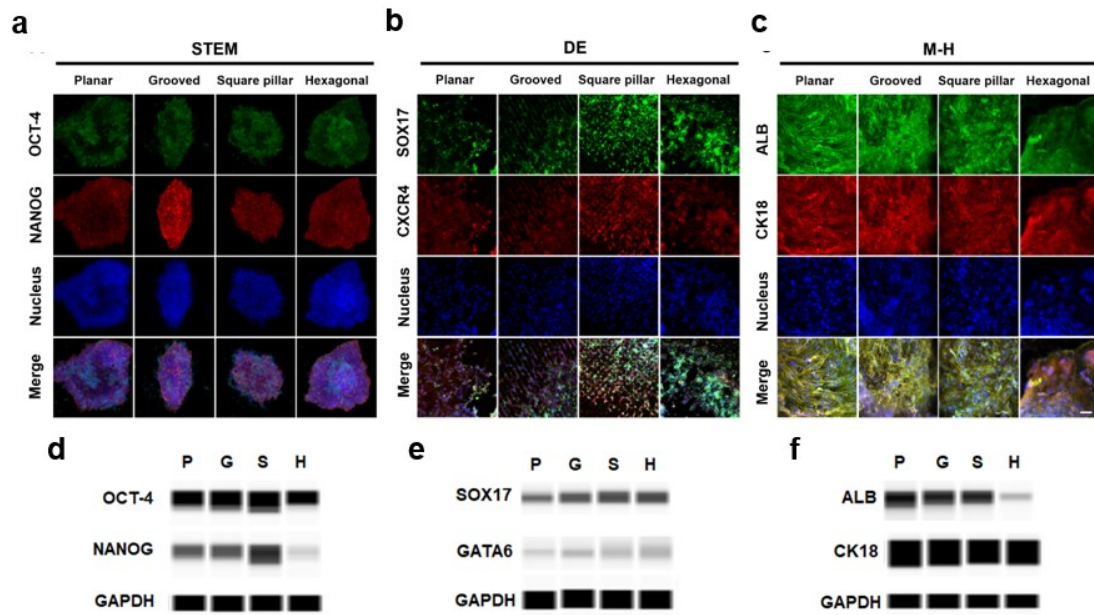


**Figure S4.** Biomarker expressions of H1 cells at different topographies on *soft* PA gel. Typical immunostaining (*1<sup>st</sup> row*) or immunoblotting (*2<sup>nd</sup> row*) images of OCT-4 and NANOG (a, d), SOX17 and CXCR4 (or GATA6) (b, e), or ALB and CK18 (c, f) were illustrated at the STEM, DE or M-H stage. Bar = 50  $\mu$ m.

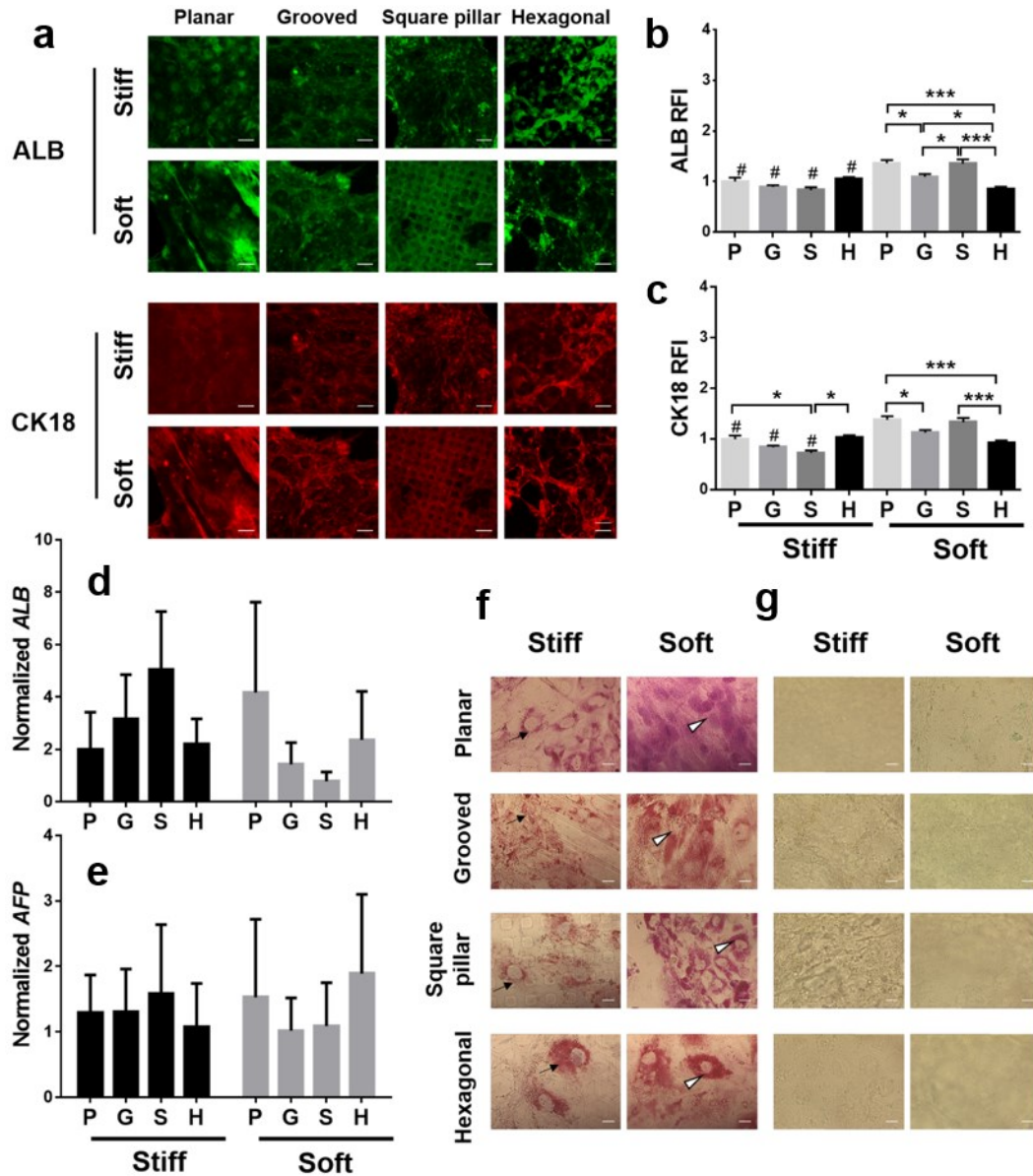


**Figure S5.** Functional tests of the differentiated H1 cells at the Pre-H stage. (a-e) Typical immunostaining images (a) and the related quantifications of ALB (b) and CK18 (c) biomarkers, as well as *ALB* (d) and *AFP* (e) gene expressions were presented. (f-g) Also plotted were the histological and histochemical staining of glycogen synthesis (f) and ICG engulfment (g). *Arrows* or *arrowheads* indicated the differences on a stiff or soft substrate, respectively. \* or \*\*\*,  $P < 0.05$  or  $0.001$  compared with the values between distinct topographies at same stiffness. #,  $P < 0.05$  compared with the values between stiff and soft substrates in same configuration (two-way ANOVA).

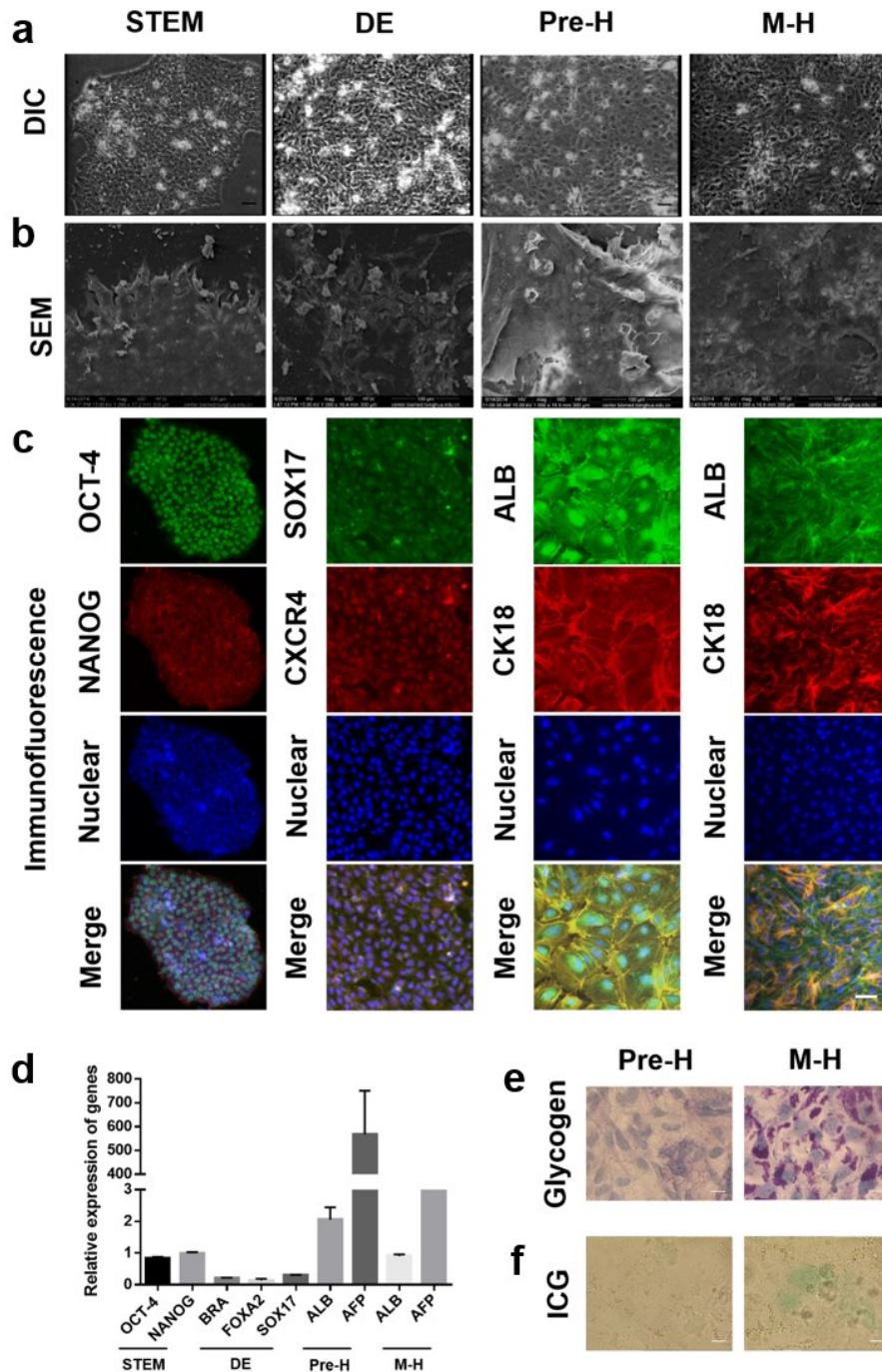


**Figure S6.** Summaries of growing H1 cells on matrigel-coated petri dish. (a-b) Typical optical (a) and SEM (b) images of H1 cells at the four stages. (c) Typical biomarker immunostaining of OCT-4 and NANOG at the STEM, SOX17 and CXCR4 at the DE, and ALB and CK18 at the Pre-H or M-H stage. Bar = 50  $\mu$ m. (d) Related gene expressions of *OCT-4* and *NANOG* at the STEM, *BRA*, *FOXA2* and *SOX17* at the DE, and *ALB* and *AFP* at the Pre-H or M-H stage. (e-f) Histological and histochemical staining of glycogen synthesis (E) and ICG engulphment (F). Bar = 50  $\mu$ m.

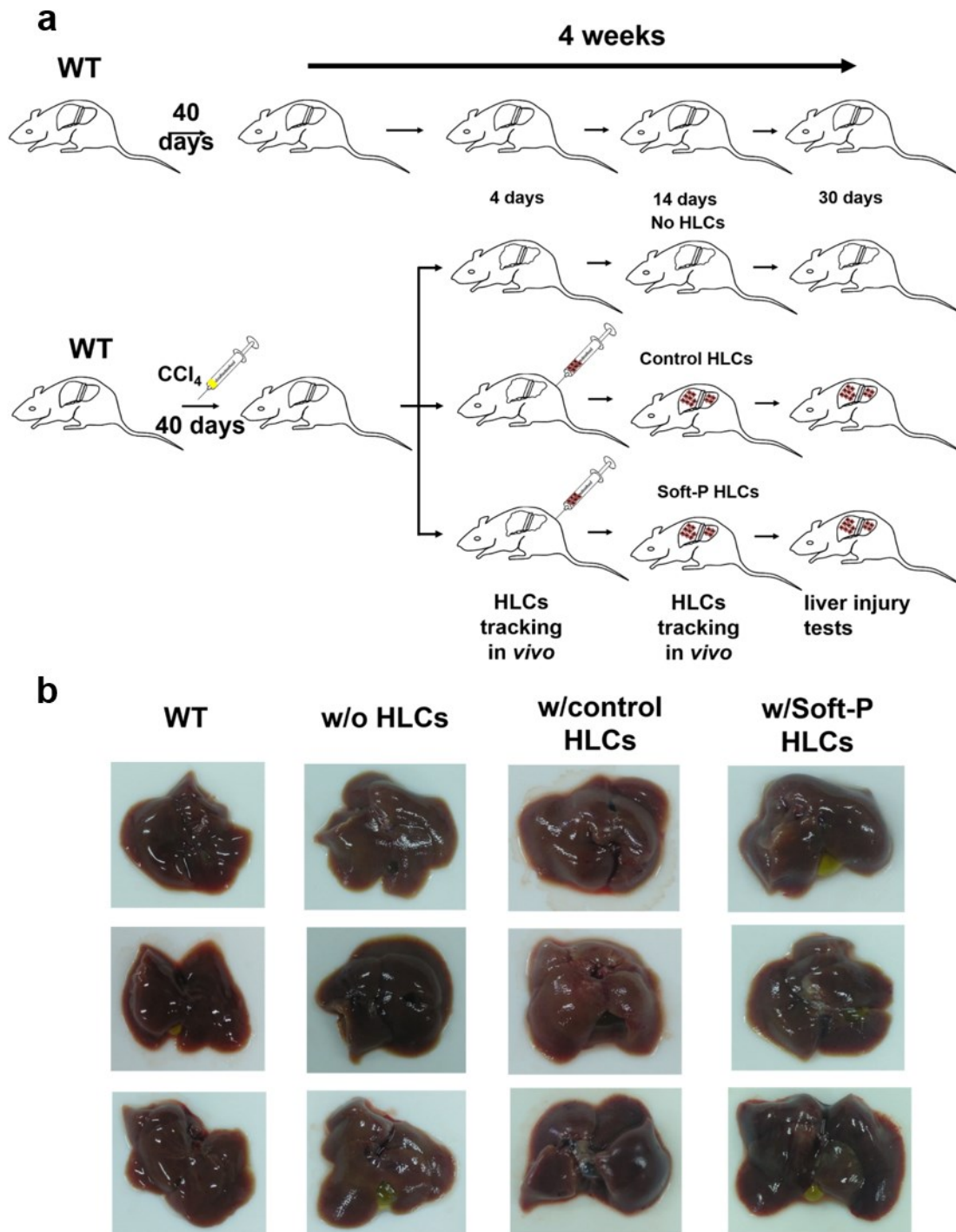


**Figure S7.** Experimental procedures and optical liver images in mice. (a) Schematic of preparing the mice with CCl<sub>4</sub>-induced liver injury and HLCs transplantation. (b) Optical liver images of WT mice, CCl<sub>4</sub>-treated mice, and CCl<sub>4</sub>-treated mice with transplanted control or Soft-P HLCs.



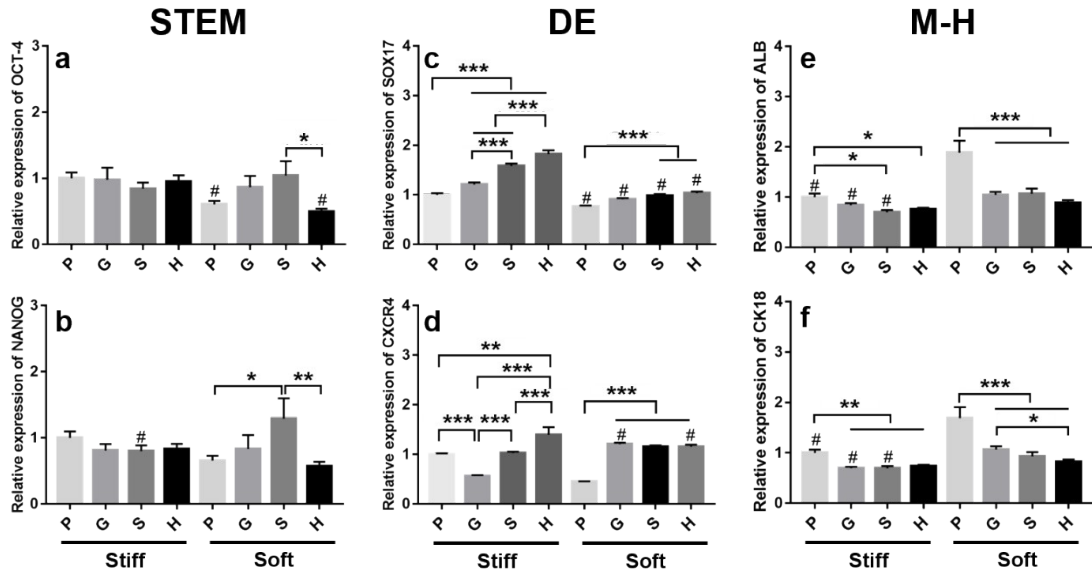


**Figure S8.** Distinct impacts of substrate topography and stiffness on pluripotency maintenance of hESCs at the Stem stage (a, b), differentiation stage-specific marker expression at the DE (c, d) and M-H stage (e, f). Relative fluorescent intensity (RFI) of two stemness biomarkers of OCT-4 (a) or NANOG (b) was quantified and presented as the mean  $\pm$  SE for > 64 clones. The RFI values of SOX17 (c) and CXCR4 (d) were quantified for > 30 fields of view (FOVs) in triplicate. Data are presented as the mean  $\pm$  SE of > 200 individual cells. The RFI values of ALB (e) and CK18 (f) were presented as the mean  $\pm$  SE for > 21 FOVs in triplicate. \*, \*\* or \*\*\*,  $P < 0.05$ , 0.01 or 0.001 compared with the values between distinct topographies at same stiffness; #:  $P < 0.05$  compared with the values between stiff and soft substrates in the respective configuration (two-way ANOVA).

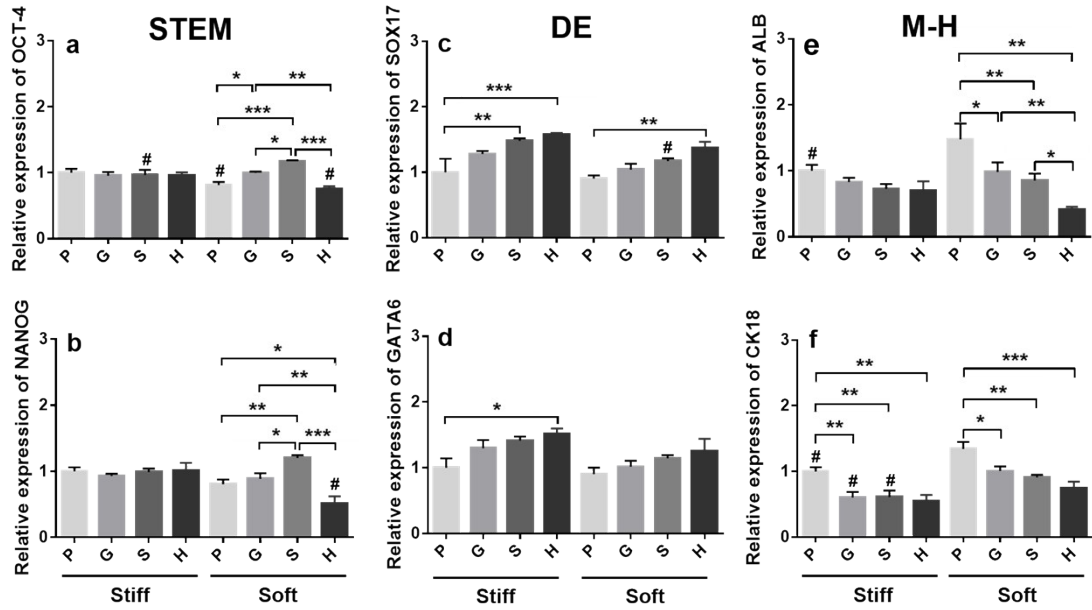


**Figure S9.** Distinct impacts of substrate topography and stiffness on pluripotency maintenance of hESCs at the Stem stage (a, b), differentiation stage-specific marker expression at the DE (c, d) and M-H stage (e, f) by Immunoblotting. Two stemness biomarkers of OCT-4 (a) or NANOG (b) was quantified and presented as the mean  $\pm$  SE from five repeats. The values of SOX17 (c) and CXCR4 (d) were quantified from five repeats. Data are presented as the mean  $\pm$  SE. The values of ALB (e) and CK18 (f) were presented as the mean  $\pm$  SE for from ten repeats. \*, \*\* or \*\*\*,  $P < 0.05$ , 0.01 or 0.001 compared with the values between distinct topographies at same stiffness; #:  $P < 0.05$  compared with the values between stiff and soft substrates in the respective configuration (two-way ANOVA).

**Table S1.** All the primer sequences and annealing temperatures for all the genes tested.

<b>Name</b>	<b>Primer sequence</b>
OCT-4	5'-GACAACAATGAAAATCTTCAGGAGA-3' 5'-TTCTGGCGCCGGTTACAGAACCA-3'
NANOG	5'-AGCCTCTACTCTTCCTACCACC-3' 5'-TCCAAAGCAGCCTCCAAGTC-3'
SOX17	TTCGTGTGCAAGCCTGAGAT TAATATACCGCGGAGCTGGC
CXCR4	AGTGATAAACACGAGGATGGCAAG TGTATATCTCCTCCCCCAAGCG
BRA	5'-CCAGGTCCCGAAAGATG-3' 5'-TGCCAAAGTTGCCAATAC-3'
FOXA2	5'-ACGACTGTTTCCTGAAGGT-3' 5'-TTGAAGGCGTAGTGGTGT-3'
GATA6	5'-CCATGACTCCAATTCCACC-3' 5'-ACGGAGGACGTGACTTCGGC-3'
ALB	AGCCTTGGTGTGATTGCCT CTCTGGTCTCACCAATCGGG
CK18	AAATCCGGGAGCACTTGGAG CAATCTGCAGAACGATGCGG
AFP	5'-TTACACAAAGAAAGCCCC-3' 5'-TCCGATAATAATGTCAGCC-3'
GAPDH	5'-GGTGAAGGTCGGAGTCAACGGA-3' 5'-GAGGGATCTCGCTCCTGGAAGA-3'
ACTIN	5'-TCACCACCACGGCCGAGCG-3' 5'-TCTCCTTCTGCATCCTGTTCG-3'

**Table S2.** Two Way ANOVA statistical tests for coupling impacts of substrate stiffness and topography<sup>†</sup>.

Source of Variation	STEM						DE						M-H								
	OCT-4			NANOG			SOX17			GATA			CXCR4			ALB			CK18		
	WES	IF	qPCR	WES	IF	qPCR	WES	IF	qPCR	WES	IF	qPCR	WES	IF	qPCR	WES	IF	qPCR			
Stiffness	0.307	0.045	0.020	0.021	0.825	<0.001	0.003	<0.001	0.092	0.008	0.926	0.780	0.193	<0.001	<0.001	<0.001	<0.001	<0.001	0.045		
Topography	<0.001	0.306	0.308	0.002	0.138	0.660	<0.001	<0.001	0.187	0.004	<0.001	0.659	<0.001	<0.001	<0.001	<0.001	<0.001	<0.001	0.067		
Stiffness $\oplus$ Topography	<0.001	0.059	0.122	<0.001	0.023	0.637	0.712	<0.001	0.836	0.827	<0.001	0.523	0.031	<0.001	<0.001	0.649	<0.001	<0.001	0.943		

<sup>†</sup>: Additional statistical data for any paired cases were not shown for clarity. For details, refer to [Figs. 5 and 6](#) with a distinct normalization of the experimental data.

□: *P* values estimated from Two Way ANOVA analysis.